



Design and Testing of a Mechanical Power Take-off System for Rolling-type Wave Energy Converter

Yichen Jiang¹ · Yuhao Peng¹ · Yuan Sun² · Zhi Zong¹ · Lei Sun¹

Received: 26 November 2019 / Revised: 26 June 2020 / Accepted: 6 August 2020 / Published online: 14 September 2020
© Korean Society for Precision Engineering 2020

Abstract

Salter's Duck can convert wave energy to mechanical energy with high efficiency up to 90%. The limitations and challenges in the usage of Salter's Duck for energy production include preventing hydraulic system from the risk of leaking hydraulic oil and removing complex huge fixed bracket. This paper presents the conceptual design and an experimental investigation of a mechanical power-take-off (PTO) system for the floating Salter's Duck. The PTO system is fully installed inside of the Salter's Duck. It consists of double counter-rotating flywheels converting the bi-directional rotation of the wave energy converter into a stable unidirectional rotation that drives a rotary generator to produce electricity. The bi-to-unidirectional function is achieved through inertial wheels, thus the novel PTO system is free of large supporting structures and hydraulic cylinders. In this paper, a detailed conceptual PTO design is proposed firstly. Further, the influence of the swing amplitude and rotation period of the wave energy converter on the power extraction efficiency is investigated. Then, the influence of the electrical load on the power-extraction efficiency is researched. In the end, the effect of the speed increasing ratio on the mechanical efficiency is examined. The experimental results show that the new type of generator mechanism can produce electricity stably.

Keywords Wave energy converter · Inertial generation device · Power extraction efficiency · Mechanical efficiency · Load characteristics

1 Introduction

1.1 Research Background

The ocean is rich in clean energy, such as wave energy, tidal energy, salt water difference energy, and temperature difference energy [1], that should be developed and utilized. In particular, ocean wave energy has the greatest potential for development. According to the forecast report published by the International Energy Organization, the amount of

available wave energy on Earth can reach 2–2.5 billion kilowatts [2–4], which far exceeds the present total global power generation. Wave energy, which is the sum of kinetic energy and potential energy of ocean waves, is the most widely distributed renewable energy source in the ocean [5, 6]. It is clean and non-polluting, and it has rich reserves, minimal environmental interference [7], and evident periodicity. The main research direction on wave energy focuses on wave power generation [8], which is sometimes used for seawater desalination [9]. Over the years, scientists and engineers have exerted considerable efforts to develop highly efficient wave power generators that can absorb, transform, and store wave energy to provide electricity for residents or supply energy to marine equipment. The large-scale commercial application of these devices can significantly improve the level of power supply and promote global economy development. It also has a considerable importance in the exploration, development, and utilization of marine resources.

Electronic supplementary material The online version of this article (<https://doi.org/10.1007/s40684-020-00253-z>) contains supplementary material, which is available to authorized users.

✉ Lei Sun
sunlei@dlut.edu.cn

¹ School of Naval Architecture Engineering, Dalian University of Technology, Dalian 116024, Liaoning, China

² State Key Laboratory of Robotics, Shenyang Institute of Automation, Chinese Academy of Sciences, Shenyang 110016, Liaoning, China

1.2 Classification and Research Status

Waves are among the numerous sources of energy, and several possible devices can be utilized to harness wave energy. These devices include floats, flaps, ramps [10], funnels [11], cylinders [12], airbags, liquid pistons [13], and “Wanshan” sharp eagle device [14]. These devices can be set at the sea surface, seabed, or anywhere in between. These can be oriented to face backward, forward, sideways, or obliquely and move in six degrees of freedom. Oil, air, water, steam, gears, or electromagnetics can be utilized for power generation [15, 16]. Such devices can create a range of demands on seabed attachments and connections to power cables. The various methods employed for these devices to survive under extreme conditions, however, are not sufficient [17]. According to the classification of the European Marine Energy Center, existing wave energy converters can be classified into six categories based on their operating principle. Four device classes account for more than 80% of research efforts: point absorbers, oscillating wave surge converters, oscillating water column, and attenuators [18, 19].

The concept of point absorber for wave energy utilization was mostly developed in the late 1970s and early 1980s in Scandinavia [20]. It is generally a wave energy converter with an oscillating body type whose horizontal dimensions are small compared to the representative wavelength. In its simplest version, the body reacts with the sea bottom. In deep water (50 m or more), the distance between the floating body and sea bottom may present difficulties. Under such a condition, multi-body systems in which the energy is converted from the relative motion between two bodies that oscillate differently [21, 22], may be used instead. This is the case of several devices currently under development, including Pelamis, Wavebob, and PowerBuoy [23].

Floating oscillating-body devices constitute a large class of wave energy converters, especially for offshore deployment in typical depths between 40 and 100 m [20, 23]. For such devices, the oscillating motion (rectilinear or angular) of a floating body or the relative motion between two moving bodies is converted into electricity by a power-take-off (PTO) system [23–25]. The research technology for the oscillating water column wave power generation device is relatively mature. This type of power generation device, however, has low power generation efficiency. To further transform and optimize it, oscillation float and pendulum-type devices have been developed. In investigating wave power generation devices, local and international research works focus on pendulum type, oscillating water column type, and floating type devices. These devices, however, have certain disadvantages. Oscillating water

column-type devices are costly, and their power generation efficiency is less than 30% [26]. The diffuse reflection type device is bulky and has inefficient underwater moving parts and low reliability. The seal of underwater differential devices is not guaranteed and easily corrodes. The point absorption type cannot work normally in bad weather [27]. The attenuator type has moving underwater parts that have low reliability and poor resistance to extreme weather. The swing-type oscillation is only applicable to shallow seas, and worse, hydraulic oil leakage from this device can cause pollution.

1.3 Rolling Wave Power Generator

The research on wave power generation has developed over the decades, and a number of different types of power generation devices have been designed to improve power generation efficiency. Existing wave generators still have certain disadvantages, such as complicated structure, high manufacturing cost, and low service life. In addition, some wave-removing devices exhibit an oscillating motion during the wave-removal process. This oscillating motion energy, which is from wave energy, is usually wasted. If the lost swing energy can be used, then the conversion efficiency of wave energy may be significantly increased. The roll-type swing power generation equipment is accordingly developed and can be classified into floating and fixed types.

In the 1970s, Salter [28] invented the duck wave energy absorption device, also known as the Salter cam, at the University of Edinburgh in Scotland, as shown in Fig. 1. The special shape of the cam, which rotates around an axis under wave action, reduces its reverse hydraulic resistance as it moves. Theoretically, the efficiency of duck-type wave power absorption can reach 90% [29, 30]. Although the primary conversion efficiency of the duck-type wave power harvester is considerably high, the internal mechanical energy conversion system of the device has always been dominated by a hydraulic system, which is extremely vulnerable, resulting in high maintenance cost and high risk of manufacturing the prototype. The application of duck-type wave energy absorption device in wave power generation is thus limited.

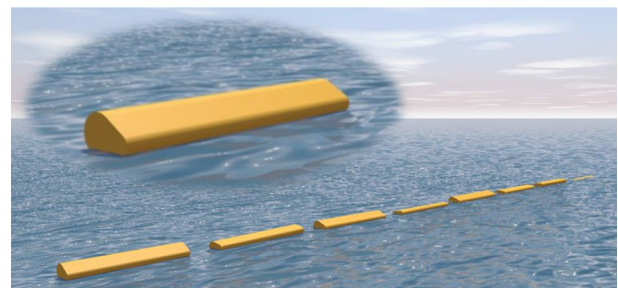


Fig. 1 Nodding duck wave power harvester

1.4 Power Take-Off System

To increase the conversion efficiency, several methods have been proposed to improve the design of the PTO system, including the motion rectifier, speed amplifier, and speed regulator [31–35]. Transmission systems can be divided into the following two separate categories: hydraulic PTO system and mechanical PTO system. The former has high efficiency but high leakage risk, high cost and difficult maintenance. The latter is simple in structure, low in cost and easy to maintain, but it cannot maintain constant generator operating speed due to wave variability. Nguyen Minh Tri [32] et al. presented a PTO system design for the point absorbers WEC, which consists of a bi-to-unidirectional gearbox, flywheel, and an electro-hydraulic actuator (EHA) that is driven by a continuously variable transmission (CVT) system. And the experiments under different working conditions were conducted to fully investigate the performance of the proposed system. The experiment results indicated that the conversion efficiency of the new PTO system was improved significantly, and the output power was smooth and stable. Tri Dung Dang et al. [33] proposed a new method to achieve the resonant behavior of a point absorber WEC using a mechanical PTO system, that is, the mass of the floating buoy was adjusted by the hydraulic flywheel accumulator system to make the natural frequency of the buoy close to the wave frequency, so that the buoy was in resonance with the wave. Tri Dung Dang et al. [34] design and tested a mechanical PTO system so-called a bidirectional rotary motion converter (BRMC), which can absorb wave energy by converting bidirectional motion of ocean waves into one-way rotation of an electric generator. The research results indicated that the efficiency of the PTO system can reach 80.4% at optimum condition including frictional loss, and the capture width ratio is up to 41.6%.

1.5 Research content

At present, a suitable power generation device that can be installed inside the rolling floating wave power plant to generate electricity is not available. In this study, design and experiments to create a new power generation device that can convert a two-way rolling motion of a float into a one-way rotational motion without a large support structure are conducted. The work is performed in the following aspects: (1) A prototype of the power generation device, whose operation is simulated in the laboratory, is designed and fabricated. (2) An experiment is conducted to demonstrate that the device can transform the periodic fluctuation of energy input into a stable power output. (3) The influence of wave swing amplitude, swing frequency, and speed ratio on the power generation performance of the power generation device is investigated and analyzed. (4) The

load characteristics of the power generation device and the mechanical characteristics of its PTO system are considered in the experiment. The test results provide an important reference for investigating the power generation performance and structural optimization of the power generation device as well as the subsequent sea tests.

2 Wave Energy Converter Design

2.1 Wave Power Harvester

In this research, a rolling wave energy absorption device, also known as a duck-type wave energy absorption device, is adopted. As shown in Fig. 1, its cross-section contour has a duck egg shape, the small round part of the front end (duckbill, duck neck, and duck belly) at the head wave surface, has a small area, and the large circle at the rear end (duck tail and duck back) at the back wave surface, has a large area. The wave power harvester swings back and forth relative to the center of the large circle at the rear end. The motion is caused by the external torque generated by the wave force and self-restoring torque. The dynamic pressure of the incident wave can effectively push the duck body to rotate around the axis, and the change in hydrostatic pressure also causes the floating part near the duckbill to make a reciprocating heave motion.

2.2 Power Generation Device Design

2.2.1 Structure

A three-dimensional (3D) view of the power generation device is shown in Fig. 2. It has 12 main components: right shaft, right one-way bearing, right inertia wheel, middle shaft, speed increaser, middle high-speed inertia wheel,

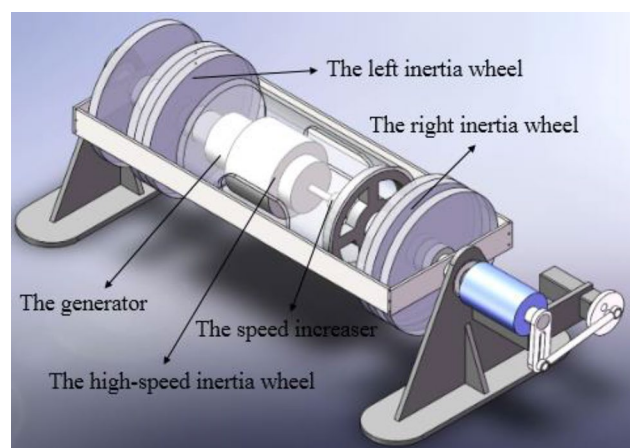


Fig. 2 3-D view of power generation device structure

middle one-way bearing, generator, left inertia wheel, left one-way bearing, left shaft, and rolling equipment. The left and right shafts are fixedly connected to the roll-type wave power harvester, and the center of the left and right shafts is the swing center of the wave power harvester. The left and right one-way bearings are nested on the left and right shafts, respectively. The left and right inertia wheels are located on the left and right one-way bearings, respectively, and the middle shaft is fixedly connected to the right inertia wheel; the middle shaft transmits the rotation to the planetary wheel speed increaser. After the speeder accelerates, the generator rotor can rotate at a high speed. The generator stator (casing) is fixedly connected to the left inertia wheel and speed increaser shell.

2.2.2 Operating Principle

The operating principle of the power device is shown in Fig. 3. In this device, the left and right shafts pass through the centers of rotation of rolling wave energy converter. A one-way bearing is installed in the inertia wheel. The left and right one-way bearings drive the left and right inertia wheels to rotate in opposite directions, respectively. When the left shaft rotates clockwise with the swinging device faster than the left inertia wheel, the left one-way bearing drives the left inertia wheel to continuously rotate clockwise. When the right shaft rotates counterclockwise with the swinging device faster than the right inertia wheel, the right one-way bearing drives the right inertia wheel to continuously rotate counterclockwise. When the left or right shaft speed is less than that of the left or right inertia wheel, the inertia wheels continue to rotate in a single direction as a result of their larger moment of inertia. The middle shaft continues to rotate counterclockwise with the right inertia wheel, and the rotational speed is transferred to the generator rotor through the planetary wheel accelerator. The planetary gear speed increaser casing and generator stator rotate clockwise with the left inertia wheel. The relative rotational speeds of the generator rotor and stator are more than twice

the original speed. Compared with the existing wave power system that only uses half the power, the power generation efficiency is therefore considerably improved.

3 Experimental Research

3.1 Rationale for Prototype Machine Fabrication

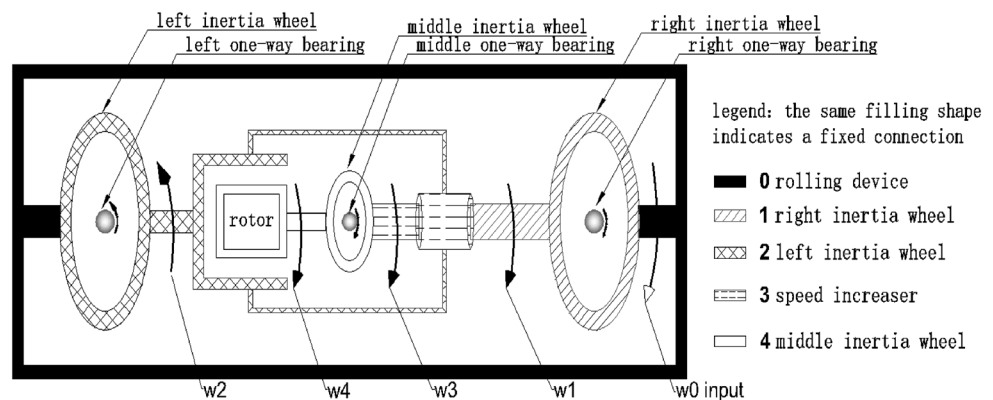
The best approach to measure the conversion efficiency of a wave-energy power generation system is by measuring the relevant parameters on site. Wave energy power generation systems are typically considerably large, and the operating environment in the sea has unfavorable conditions. In view of these, obtaining all the relevant parameters of the actual accurate measuring system even with the use of current technical approaches is extremely difficult. Before developing and building the entire wave power generation system, a prototype machine should therefore be designed, manufactured, and tested. Thereafter, the conversion efficiency of the prototype should be measured and calculated. Finally the comprehensive performance of the wave power generation equipment, which provides basic data for subsequent research, should be effectively evaluated. At present, the method of combining laboratory and field tests is used to comprehensively evaluate the conversion efficiency of the wave power generation system.

3.2 Method for Simulating Duck-type Floating Body Swing

In this experiment, a motion conversion device composed of the servo motor and linkage mechanism is designed. The conversion device can effectively simulate the operating status of the duck-type floating body at different swing amplitudes and frequencies to explore the influence of various factors on the performance of the power generation device.

As shown in Fig. 4, the linkage mechanism connects the servo motor and torque sensor. It can convert the uniform

Fig. 3 Operating principle of power device



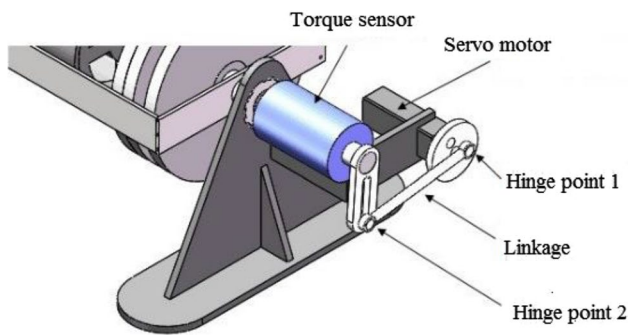


Fig. 4 Linkage mechanism design

rotation of the servo motor into the reciprocating oscillation of the center shaft of the torque sensor to simulate the swing motion of the rolling wave power harvester. The oscillating amplitude of the rolling wave power plant can be adjusted by changing the distance from the center of hinge point 1 to the rotation axis of the servo motor and the distance from hinge point 2 to the rotation axis of the torque sensor. The swinging frequency of the rolling wave generator can be adjusted by controlling the speed of the servo motor. Based on the foregoing method, the linkage mechanism can therefore be used to simulate the regular-motion operating state of the rolling wave power generation equipment at different swing amplitudes and frequencies. It is worthy to note that this driving system cannot imitate the irregular motion response of a rolling-type wave energy converter under the irregular sea states. Under the scope of this work, it is applied to understand and obtain the influences of different design parameters of the power-take-off system on the power generation performance.

3.3 Experimental Model

The experimental equipment and instruments mainly include the Ablesino torque sensor, dynamic motion attitude recorder (gyroscope), Nosaixis data acquisition instrument, HZK PZ9902U AC/DC electrical parameter measuring instrument, Senring spectrum conductive slip ring, 60-G01330 servo motor, H3N-DD drive, TC5510 motion control system, alternator, dual-axis planetary speed increaser PLS56, 1000- Ω pure resistance, and linkage mechanism.

The torque sensor, which has a limit of 50-N·m and 0.5% accuracy, is employed to measure the torque (mechanical input torque) of the left and right shafts. The one-channel Nosaixis data acquisition instrument, which has a sampling frequency of 1000 Hz, is used to collect and analyze the torque sensor signal. The swing angular velocity (mechanical input speed) of the simulated duck-type floating body is measured using the dynamic motion attitude recorder (gyroscope), which has a 100-Hz sampling frequency. The



Fig. 5 Prototype of power generation device

AC/DC parameter meter is installed at each loaded end of the device to collect and measure the voltage, current, and electric power of generator output.

The test objectives are as follows: (1) verify the feasibility of stable power generation using the internal power generation device of the new rolling wave power generation equipment; (2) determine the laws between the electric power and power generation efficiency of the new generation device and the simulated swing amplitude and frequency of the rolling wave generation device; (3) study the characteristics of the alternator in the new generation device and obtain its characteristic curve; (4) investigate the effect of different loads on the power generation and efficiency of the new power generation device and thereafter obtain its optimal matching load; (5) examine the mechanical characteristics of the power generation device and obtain the rule between its mechanical efficiency and speed increaser ratio.

The prototype of the power generation device is designed and manufactured according to the operating principle. As shown in Fig. 5, the right end of the power generating device is mounted on a fixed platform to fix the torque sensor and servo motor. The left end of the torque sensor shaft is fixedly connected to the right rotating shaft of the power generating device. The torque sensor is used to measure the mechanical input torque of the rolling wave energy absorbing device. The torque signal is therefore transmitted to the computer through the Nosaixis data acquisition instrument. The dynamic motion attitude recorder (gyroscope) is fixed on the horizontal bar of the simulated duck-type floating body and is used to measure the swing amplitude, swing frequency, and swing speed of the rolling wave energy absorbing equipment. The motion angle, velocity, and acceleration signal are directly transmitted to the computer through the gyroscope. The output end of the generator is connected to the input end of the AC/DC parameter-measuring instrument through the rectifier bridge, and the output end of the

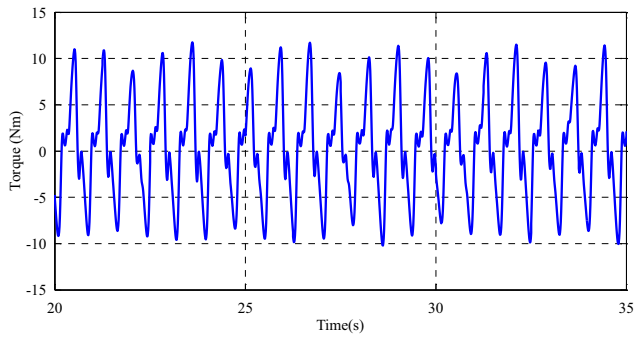


Fig. 6 Typical time series of mechanical input torque

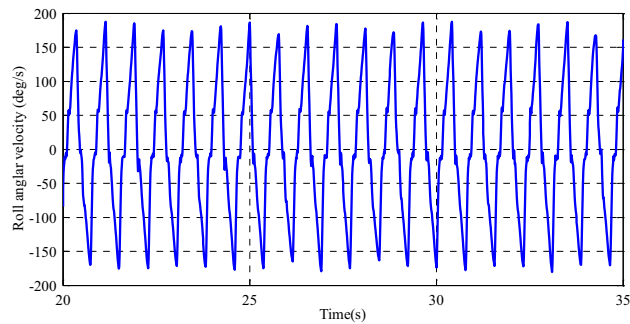


Fig. 7 Typical time series of mechanical input speed

AC/DC parameter-measuring instrument is connected with a pure resistance to collect the voltage and electric power data of the generator. The main parameters of the power generator prototype are as follows: the moments of inertia of the left and right inertia wheels are 1.01 and 0.757 kg m², respectively; the rated power of the generator is 30 W.

4 Results and Discussion

4.1 Mechanical Input and Electrical Output

The characteristics of the mechanical input torque and speed, electrical output voltage, and electric power are investigated, and the efficiency of the internal power generation device is explored in the laboratory to verify the stable power generation feasibility of the device. A set of experimental data is selected for detailed analysis under operating conditions where the swing amplitude, frequency, load resistance, and speed increaser ratio are 35.2°, 1.32 Hz, 1000 Ω, and 13, respectively. The mechanical input torque and speed illustrated in Figs. 6 and 7 exhibit periodic fluctuations with time, and their cycles are consistent with the swing frequency (0.758 s). Small irregular fluctuations between the peaks and troughs of mechanical input torque and speed are

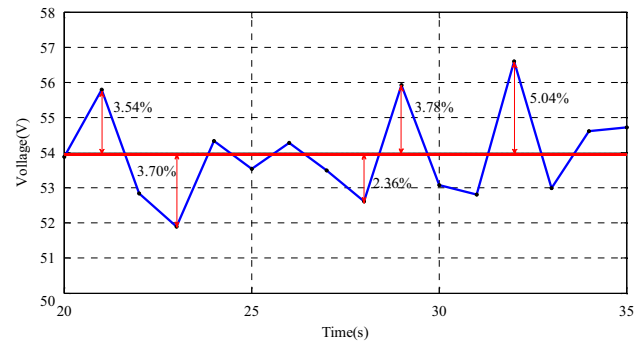


Fig. 8 Typical time series of output voltage

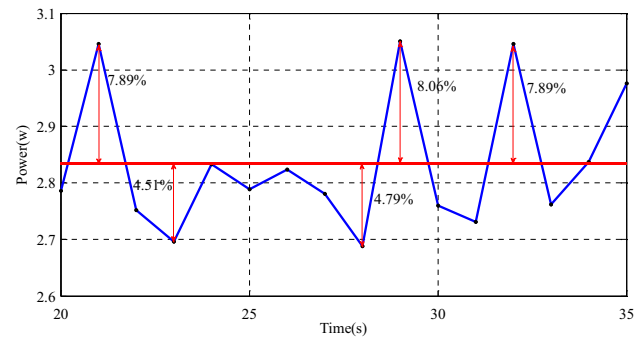


Fig. 9 Typical time series of output electric power changes over time

caused by the mechanical error of the power transmission converter.

As shown in Figs. 8 and 9, while the mechanical input torque and speed change more intensely with time, the output voltage and electric power curves remain relatively flat over time. The above phenomenon occurs because of the mechanical energy storage wheel in the wave power generation device that has been designed to store and release energy. It performs an important function in cutting crests and filling troughs. The maximum instantaneous electric power is 3.051 W, and the minimum is 2.696 W; hence, the maximum electric power fluctuation rate is 8.06%. The calculated maximum voltage fluctuation rate is 5.04%, and the maximum and minimum instantaneous voltages are 55.92 and 51.89 V, respectively. In the past, the voltage and electric power volatility of wave power generation devices is generally high. It is evident that the performance of such a power generation device is considerably stable compared to previous devices. There is no significant fluctuation in voltage and electric power, and the safety of the battery, voltage stabilization module device, and electric load are thus protected.

The new power generation device can output stable voltage and power. It will therefore have less impact when incorporated into the power grid and is more likely to transmit the

generated electricity to users through the power grid system. The foregoing fully reflects the potential practical value of the new power generation device.

4.2 Calculation Method for Power Generation Efficiency

The power generation efficiency cannot be directly determined because of the difficulty in measuring the correct input power [36]. The torque sensor and gyroscope measure the angular velocity and applied torque from which the mechanical input power can be calculated. There is a minimal friction loss, however, in the joint surface between the right shaft and torque sensor.

In this study, to calculate the average power generation efficiency of the internal power generation device, the measured data during the 15-s period after the internal power generation device has been operating for 20 s are employed. It is calculated as follows:

$$\eta = \frac{\sum P_i}{\sum T_i \omega_i} \quad (1)$$

where η is the average power generation efficiency, T is the mechanical input torque, ω is the mechanical input angular velocity, and P is the output electrical power.

Based on the above formula, the power generation efficiency of the internal power generation device is 24.16% under operating conditions in which the swing amplitude, swing frequency, load resistance, and speed increaser ratio are 35.2°, 1.32 Hz, 1000 Ω , and 13, respectively.

4.3 Effect of Swing Frequency on Power Generation Efficiency

In order to investigate the effect of driving swing frequency on the power generation efficiency of the internal power generation device, experimental data are measured under operating conditions where the driving swing amplitude is 35.20° and driving swing frequencies are 0.98, 1.08, 1.16, 1.24, 1.32, and 1.40 Hz.

The influence of swing frequency on power generation efficiency under operating conditions where the swing amplitude is 35.20°, is shown in Fig. 10. It can be observed that the power generation efficiency is relatively linear with the swing frequency. At a large swing frequency, the voltage and current frequency are larger, and the magnitude of the inductive part of the power generation device impedance is increases; consequently, power generation efficiency improves. Based on the analysis of experimental principles and data, the relationship between power generation efficiency and swing frequency can be summarized as

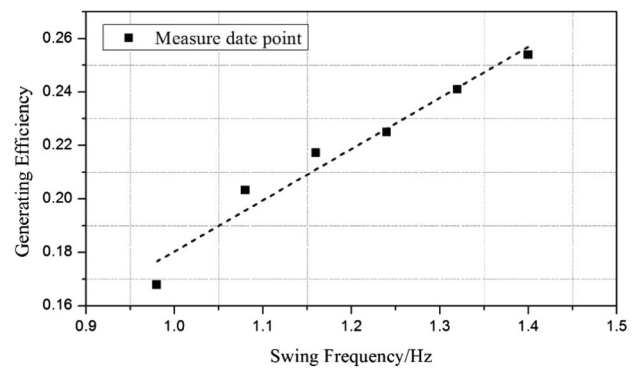


Fig. 10 Power generation efficiency at various swing frequencies

$$\eta = \alpha_1 F + \beta_1 \quad (2)$$

where η is the power generation efficiency, α_1 is the coefficient related to swing amplitude, β_1 is the coefficient related to swing frequency, and F is the swing frequency. The experimental data are analyzed using the multiple linear regression of the least square method. The mathematical relationship between power generation efficiency and swing frequency is thereafter obtained under the condition that the moments of inertia of the inertia wheel and alternator are the same, the speed increaser ratio is 13, and the swing amplitude is 35.2°.

$$\eta = 0.19136F - 0.01096 \quad (3)$$

4.4 Effect of Swing Amplitude on Power Generation Efficiency

With the objective of investigating the effect of driving swing amplitude on the power generation efficiency of the internal power generation device, experimental data are measured in the laboratory under operating conditions where the driving swing frequency is 1.32 Hz and driving swing amplitudes are 22.40°, 26.01°, 35.20°, 40.54°, 45.20°, and 50.48°.

Figure 11 shows the influence of swing amplitude on power generation efficiency under operating conditions where the swing frequency is 1.32 Hz. It can be observed that the power generation efficiency exhibits an increasing trend with the increase in swing amplitude, and thus have a linear relationship. The power generation efficiency improves because large amplitudes impart higher speeds to the power generation device. After a more detailed analysis of experimental principles and data, the relationship between power generation efficiency and swing amplitude can be summarized as

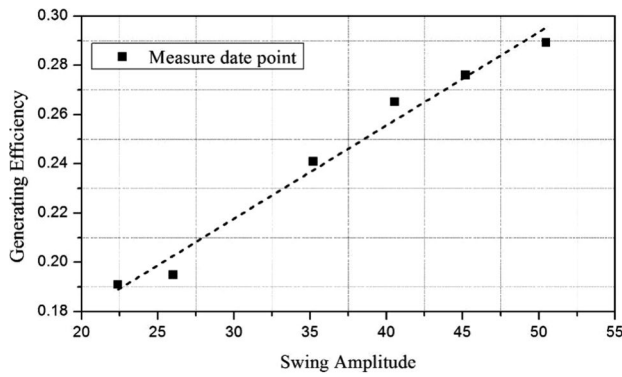


Fig. 11 Power generation efficiency at various swing amplitudes

$$\eta = \alpha_2 A + \beta_2 \tag{4}$$

where η is the power generation efficiency, α_2 is the coefficient related to swing frequency, β_2 is the coefficient related to swing amplitude, and A is the swing amplitude. Utilizing the same method, the mathematical relationship between power generation efficiency and swing amplitude is obtained under the condition that the moments of inertia of the inertia wheel and alternator are the same, the speed increaser ratio is 13, and the swing frequency is 1.32 Hz.

$$\eta = 0.00379A + 0.10418 \tag{5}$$

4.5 Effect of Swing Frequencies on Power Generation at Different Swing Amplitudes

As the input and output powers are time varying, the power shown in Fig. 12 is the average power over 15 periods after the transient state. For a monochromatic sine input and resistive generator load, the peak power is approximately achieved during the periods of maximum velocity during the rise and fall between the wave trough and crest.

Figure 12 clearly shows that the output power linearly increases with the swing frequency. At high frequencies, the speed of the power generation device is high, which improves the output power. According to the analysis of experimental principles and data, the relationship between power generation and swing frequency at different swing amplitudes can be summarized as

$$P = \alpha F + \beta A + \lambda \tag{6}$$

where P is the electric power; α is the coefficient related to swing amplitude; F is the swing frequency; β is the coefficient related to swing frequency; A is the swing amplitude; λ denotes the coefficient related to the inertia of inertia wheel, speed increase ratio, and motor damping. After the

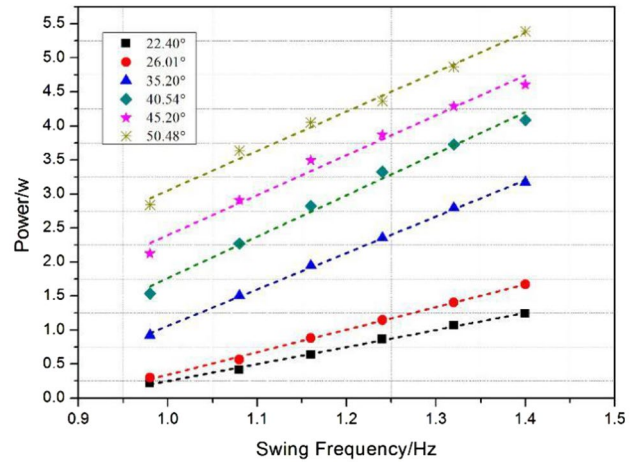


Fig. 12 Variation of output power with swing frequency at different swing amplitudes

experimental data analysis using the multiple linear regression of the least square method, the mathematical relationship between power generation, swing amplitude, and frequency is obtained under the condition that the moments of inertia of the inertia wheel and alternator are the same, and the speed increaser ratio is 13.

$$P = 1.2316F + 0.17052A - 5.0979 \tag{7}$$

4.6 Repeatability Test Research on Power Generation Experiment

In order to verify the repeatability of the power generation experiment of the novel power generation device, three repeated experiments are performed under six sets of operating conditions. The experimental data shown in Fig. 13 are measured three times under operating conditions where

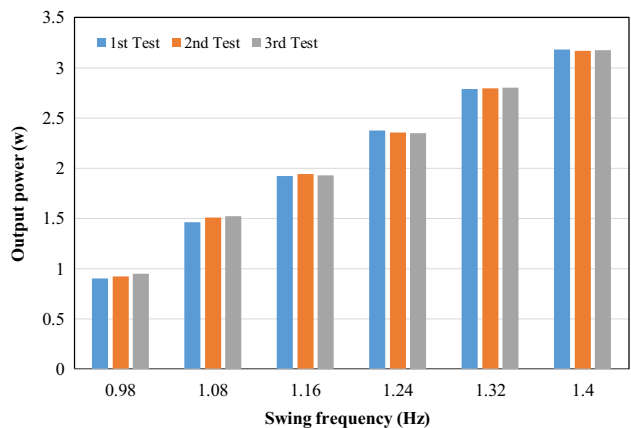


Fig. 13 Output power under six operating conditions in three repeated experiments

Table 1 Values of relative deviation in output power

Swing frequency (Hz)	1st relative deviation	2nd relative deviation	3rd relative deviation
0.98	-0.0272	0.0000	0.0258
1.08	-0.0231	0.0058	0.0165
1.16	-0.0047	0.0071	-0.0025
1.24	0.0060	-0.0018	-0.0042
1.32	-0.0027	0.0001	0.0026
1.40	0.0013	-0.0018	0.0005

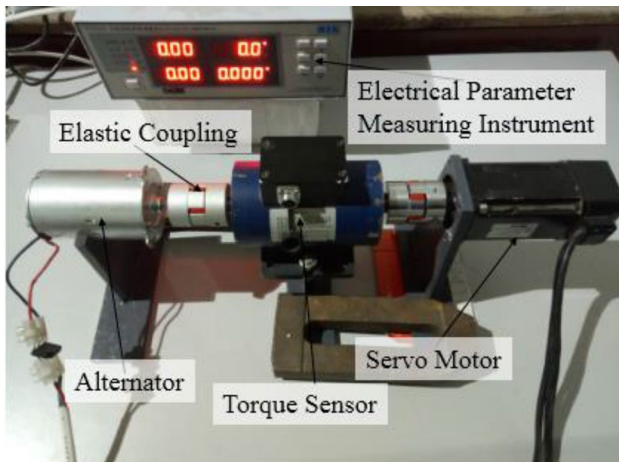


Fig. 14 Alternator characteristic test device

the swing amplitude is 35.2°, the speed increaser ratio is 13, load resistance is 1000 Ω, and swing frequencies are 0.98, 1.08, 1.16, 1.24, 1.32, and 1.40 Hz.

The relative deviation is used to analyze the data error of the three repeated experiments. This deviation refers to the ratio of the difference between a single data value and data mean to the data mean.

Table 1 summarizes the information in Fig. 13 which show the relative deviation under each condition in the three repeated experiments. Based on the table, the relative deviations of the output power in the three experiments are less than ± 3%, which proves that the experiment on the novel power generation device has considerably high repeatability.

4.7 Experimental Research on Generator Characteristics

In this experiment, the generator in the novel power generation device is tested to investigate its characteristics. The experimental device consists of the servo motor, elastic coupling, torque sensor, alternator, and electric parameter measuring instrument, as shown in Fig. 14. The torque sensor measures the torque and speed of the alternator input. The

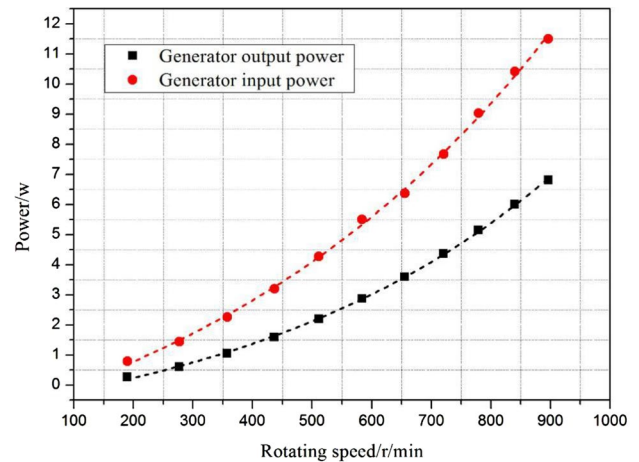


Fig. 15 Input power and output power at various rotational speeds

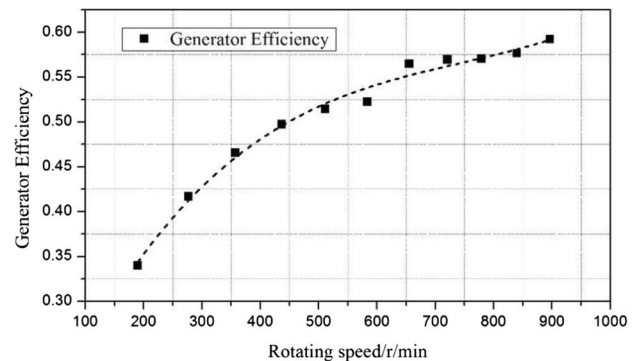


Fig. 16 Generator efficiency at various rotational speeds

power and voltage of the alternator output are measured and collected using an electric parameter measuring instrument.

With the purpose of examining the influence of rotor speed on alternator efficiency and electric power, the experimental data are measured at rotor speeds of 189.7, 277.2, 357.6, 436.7, 511.6, 583.9, 655.6, 720.8, 779.2, 840.3, and 896.6 r/min.

Figure 15 shows a non-linear trend with a moderate increase in incremental output power as rotational speed increases, the input power intensifies at a higher rotational speed, and the growth rate moderately increases gradually. At a high rotational speed, the induced electromotive force of the generator increases, which improves the output power.

Figure 16 shows that as the rotational speed increases, the generator efficiency increases non-linearly with a growth trend that gradually decreases, indicating that there is an ultimate generator efficiency. To explain this, note that the generator efficiency is the ratio of the output electric power to the input power. The output power and input power increase with the increase in rotational speed, but that growth rate of

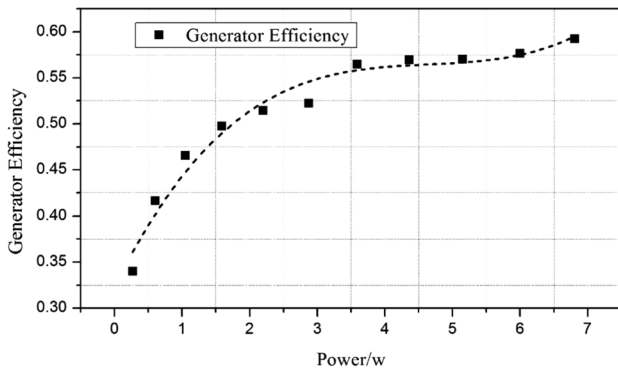


Fig. 17 Relationship between generator efficiency and generator output power

the input power is faster than that of the output power. As a result, the growth rate of generator efficiency decreases.

Figure 17 shows a nonlinear trend with a moderate decrease in incremental generator efficiency as the rotational speed increases. The generator efficiency continues to increase because the generator does not reach the rated speed of 3000 rpm. Based on the detailed analysis of the experimental principle and data, the mathematical relationship between generator’s power generation efficiency and output power is derived as

$$\eta = 0.0023P_o^3 - 0.0314P_o^2 + 0.1493P_o + 0.323 \quad (8)$$

where η is the generator efficiency, and P_o is the generator output power.

4.8 Experimental Research on Load Characteristics

Under operating condition where the swing amplitude is 35.20°, swing frequency is 1.24 Hz, and speed increaser ratio is 13 is selected for the experiment. The experimental data are measured at load resistances of 100, 200, 280, 400, 470, 620, 680, 750, 880, 1000, 1100, 1200, 1300, 1400, 1500, 1700, 1800, and 2000 Ω. After investigating the load characteristics of the new power generation device, the optimum matching load can be obtained.

The mechanical input power of the power generation device decreases with the increase in load, as shown in Fig. 18. The trace shows a linear decrease when the load resistance is less than 880 Ω, and the downward trend gradually decreases when the load resistance is greater than 880 Ω. The output power of the device initially increases and thereafter decreases with the continuous load. This indicates that the output electric power has a maximum value, and the load corresponding to the maximum value is the optimal load of the output power of the device.

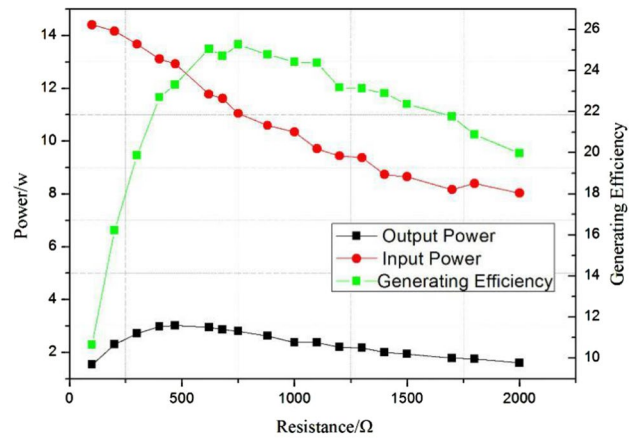


Fig. 18 Input power, output power, and generation efficiency at various loads

The figure clearly shows that the efficiency of the power generation device initially increases rapidly. It thereafter tends to be stable, and finally gradually decreases with the continuous load. This indicates that the power generation efficiency is higher in a relatively stable region, and the load region corresponding to the smoother region is the best matching load region for the efficiency of the device.

4.9 Experimental Research on Mechanical Properties

The effect of the speed increaser ratio on mechanical efficiency can be determined by analyzing the mechanical characteristics of the novel power generation device.

To investigate the relationship between the mechanical efficiency and speed increaser ratio, the experimental data are measured under conditions where the speed increaser ratios are 5.3, 13, and 18; the swing frequencies are 0.98, 1.08, 1.16, 1.24, 1.32, and 1.40 Hz, and the swing amplitudes are 22.40°, 26.01°, 35.20°, 40.54°, 45.20°, and 50.48°, respectively.

As shown in Fig. 19, the mechanical efficiency of the power generation device increases with the continuous output power. The growth trend gradually decreases and finally tends to become stable. This indicates that as the output power increases, its effect on the mechanical efficiency gradually decreases, and when the output power reaches a certain value, its increase has a minimal effect on the mechanical efficiency. When the output power is constant, the mechanical efficiency with speed increaser ratios of 13 and 18 are significantly higher than that with a speed increaser ratio of 5.3. The mechanical efficiency with a speed increaser ratio of 18 is slightly lower than that with a speed increaser ratio of 13. When the speed increaser ratios are 13, 5.3, 18, the maximum limits of mechanical efficiency are approximately 50%,

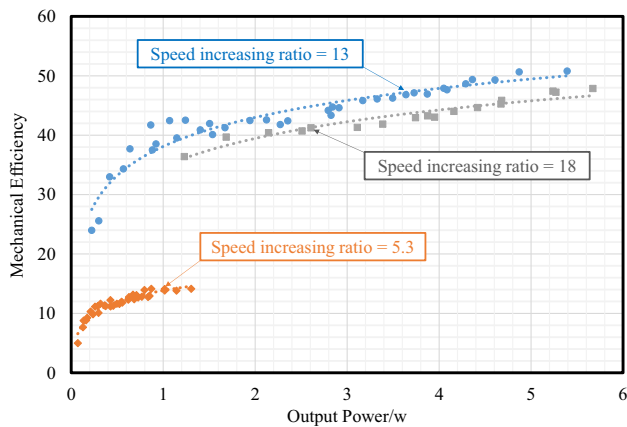


Fig. 19 Variation of mechanical efficiency with output power at three speed increaser ratios

15%, and 48%, respectively. Based on the above analysis, it is not necessary for the speed increaser ratio in the device to reach the largest value because the mechanical efficiency would decrease if the speed increaser ratio is excessively large. Apparently, the mechanical efficiency has a matching optimal speed increaser ratio. A more detailed analysis would determine the extent to which the speed increaser ratio has to be optimized according to the mechanical properties relative to friction; hence, this can be a good topic for future research.

5 Conclusion

Based on the analysis of experimental data, the conclusions drawn are as follows:

1. The experimental results show that the novel power generation device for ocean energy applications proposed in this paper can effectively transform periodic mechanical energy input into a stable power output. The design of mechanical energy storage wheel enables it to perform energy storage and release functions. These functions, which are important in cutting peaks and filling valleys, accordingly reduces the fluctuation rates of electric power and voltage in the wave power generation system by 8.06% and 3.78%, respectively.
2. The power generation efficiency of the device has a relatively linear relationship with the swing amplitude and frequency.
3. The efficiency of the generator inside the power generation device has a nonlinear relationship with the rotational speed. It exhibits a moderate decrease in incremental efficiency with increasing rotational speed.
4. The power generation device has the best matching load. The optimal load resistance of the device is approxi-

mately 500 Ω , and the optimal load resistance area for the power generation efficiency is 600–900 Ω .

5. The mechanical efficiency of the power generation device has an optimal matching speed increaser ratio. When the speed increaser ratio is 13, the maximum mechanical efficiency achieved is approximately 50%.

Acknowledgements The present work is supported by Qingdao National Laboratory for Marine Science and Technology (QNL-M2016ORP0402); and the State Key Laboratory of Robotics (No. 2019-O19). The authors would like to thank their support.

Funding This research was funded by Qingdao National Laboratory for Marine Science and Technology (QNL-M2016ORP0402) and the State Key Laboratory of Robotics (No. 2019-O19).

Compliance with Ethical Standards

Conflict of Interest The authors declare no conflict of interest.

References

1. Yin-Bei, D., & Wen, X. (2004). Development and utilization of ocean energy. *Renewable Energy*, 38(8), 1811–1820.
2. Bastien, S. P., Sepe, R. B., Grilli, A. R., Grilli, S. T., & Spaulding, M. L. (2009). Ocean wave energy harvesting buoy for sensors. Energy Conversion Congress and Exposition, 2009. ECCE 2009. IEEE. IEEE.
3. Orazov, B., O'Reilly, O. M., & Savaş, Ö. (2010). On the dynamics of a novel ocean wave energy converter. *Journal of Sound and Vibration*, 329(24), 5058–5069.
4. Aoun, N. S., Harajli, H. A., & Queffeuilou, P. (2013). Preliminary appraisal of wave power prospects in Lebanon. *Renewable Energy*, 53, 165–173.
5. Mueller, M. A. (2002). Electrical generators for direct drive wave energy converters. *IEE Proceedings-generation, transmission and distribution*, 149(4), 446–456.
6. Berrie, T. W. (1967). The economics of system planning in bulk electricity supply. *Electrical Review*, 22, 425–428.
7. López, I., Andreu, J., Ceballos, S., de Alegría, I. M., & Kortabarria, I. (2013). Review of wave energy technologies and the necessary power-equipment. *Renewable and sustainable energy reviews*, 27, 413–434.
8. Khan, N., Kalair, A., Abas, N., & Haider, A. (2017). Review of ocean tidal, wave and thermal energy technologies. *Renewable and Sustainable Energy Reviews*, 72, 590–604.
9. Hicks, D. C., Pleass, C. M., & Mitcheson, G. R. (1988). Delbuoy: Wave-powered seawater desalination system. In OCEANS'88. 'A Partnership of Marine Interests'. Proceedings (pp. 1049–1054). IEEE.
10. Liu, Z., Shi, H., Cui, Y., & Kim, K. (2017). Experimental study on overtopping performance of a circular ramp wave energy converter. *Renewable Energy*, 104, 163–176.
11. Zhang, Z. Y., Liu, H. X., Zhang, L., Zhang, W. C., & Ma, Q. W. (2018). Study on the performance analysis and optimization of funnel concept in wave-energy conversion. *Journal of Marine Science and Technology*, 23(3), 696–705.
12. Cai, S. G., Ouahsine, A., & Sergent, P. (2016). Modelling wave energy conversion of a semi-submerged heaving cylinder. In

- Computational Methods for Solids and Fluids (pp. 67–79). Springer, Cham.
13. Vakis, A. I., & Anagnostopoulos, J. S. (2016). Mechanical design and modeling of a single-piston pump for the novel power take-off system of a wave energy converter. *Renewable Energy*, 96, 531–547.
 14. Sheng, S., Wang, K., Lin, H., Zhang, Y., You, Y., Wang, Z., et al. (2017). Model research and open sea tests of 100 kW wave energy converter Sharp Eagle Wanshan. *Renewable Energy*, 113, 587–595.
 15. Cruz, J. (2007). *Ocean wave energy: current status and future perspectives*. New York: Springer Science & Business Media.
 16. Falnes, J. (2007). A review of wave-energy extraction. *Marine Structures*, 20(4), 185–201.
 17. Salter, S. (2016). Wave energy: Nostalgic Ramblings, future hopes and heretical suggestions. *Journal of Ocean Engineering and Marine Energy*, 2(4), 399–428.
 18. Magagna, D., & Uihlein, A. (2015). Ocean energy development in Europe: Current status and future perspectives. *International Journal of Marine Energy*, 11, 84–104.
 19. Lehmann, M., Karimpour, F., Goudey, C. A., Jacobson, P. T., & Alam, M. R. (2017). Ocean wave energy in the United States: Current status and future perspectives. *Renewable and Sustainable Energy Reviews*, 74, 1300–1313.
 20. Antonio, F. D. O. (2010). Wave energy utilization: A review of the technologies. *Renewable and sustainable energy reviews*, 14(3), 899–918.
 21. Yang, S. H., Wang, Y. Q., He, H. Z., Zhang, J., & Chen, H. (2018). Dynamic properties and energy conversion efficiency of a floating multi-body wave energy converter. *China Ocean Engineering*, 32(3), 347–357.
 22. Prakash, S. S., Mamun, K. A., Islam, F. R., Mudliar, R., Pau'u, C., Kolivuso, M., & Cadralala, S. (2016, December). Wave energy converter: a review of wave energy conversion technology. In 2016 3rd Asia-Pacific World Congress on Computer Science and Engineering (APWC on CSE) (pp. 71–77). IEEE.
 23. Zhang, X. T., Yang, J. M., & Xiao, L. F. (2016). An oscillating wave energy converter with nonlinear snap-through power-take-off systems in regular waves. *China Ocean Engineering*, 30(4), 565–580.
 24. Zhang, Y. Q., Sheng, S. W., You, Y. G., Wu, B. J., & Liu, Y. (2014). Research on energy conversion system of floating wave energy converter. *China Ocean Engineering*, 28(1), 105–113.
 25. Zhang, D. H., Li, W., Zhao, H. T., Bao, J. W., & Lin, Y. G. (2014). Design of a hydraulic power take-off system for the wave energy device with an inverse pendulum. *China Ocean Engineering*, 28(2), 283–292.
 26. Energy, A. (2005). Oscillating water column wave energy converter evaluation report. The Carbon Trust, Marine Energy Challenge, pp. 1–196.
 27. Zheng, X. B., Jiang, J., & Zhang, L. (2013). Power characteristic analysis and optimization of point absorber wave energy converter. *Applied mechanics and materials* (Vol. 313, pp. 837–842). Zurich: Trans Tech Publications.
 28. Salter, S. H. (1974). Wave power. *Nature*, 249(5459), 720–724.
 29. Salter, S. H. (1992, October). The swinging mace. In Proceedings of Workshop Wave Energy R&D, Cork, Ireland (pp. 197–206).
 30. Sakai, K., Kashiwagi, M., & Takaramoto, R. (2014). Wave-energy absorption by a rotating electric-power generator set inside an asymmetric floating body. *Journal of the Society of Naval Architects of Japan*, 19, 205–211.
 31. Choi, K. S., Yang, D. S., Park, S. Y., & Cho, B. H. (2012). Design and performance test of hydraulic PTO for wave energy converter. *International Journal of Precision Engineering and Manufacturing*, 13(5), 795–801.
 32. Tri, N. M., Binh, P. C., & Ahn, K. K. (2018). Power take-off system based on continuously variable transmission configuration for wave energy converter. *International Journal Precision Engineering Manufacturing-Green Technology*, 5(1), 103–110.
 33. Dang, T. D., Nguyen, M. T., Phan, C. B., & Ahn, K. K. (2019). Development of a wave energy converter with mechanical power take-off via supplementary inertia control. *International Journal of Precision Engineering and Manufacturing-Green Technology*, 6(3), 497–509.
 34. Dang, T. D., Phan, C. B., & Ahn, K. K. (2019). Modeling and experimental investigation on performance of a wave energy converter with mechanical power take-off. *International Journal of Precision Engineering and Manufacturing Green Technology*, 6(4), 751–768.
 35. Dang, T. D., Phan, C. B., & Ahn, K. K. (2019). Design and investigation of a novel point absorber on performance optimization mechanism for wave energy converter in heave mode. *International Journal of Precision Engineering and Manufacturing Green Technology*, 6, 477–488. <https://doi.org/10.1007/s40684-019-00065-w>.
 36. Prudell, J., Stoddard, M., Amon, E., Brekken, T. K., & Von Jouanne, A. (2010). A permanent-magnet tubular linear generator for ocean wave energy conversion. *IEEE Transactions on Industry Applications*, 46(6), 2392–2400.

Publisher's Note Springer Nature remains neutral with regard to jurisdictional claims in published maps and institutional affiliations.



Yichen Jiang is an Associate Professor at the Dalian University of Technology. He received his Ph.D. (2014) in Mechanical Engineering/Ocean Engineering from the University of California at Berkeley. His research interests include: marine hydrodynamics, ocean renewable energy, highperformance vessels, and computational fluid dynamics.



Yuhao Peng received his Bachelor's degree in Marine Engineering from Dalian Maritime University, China in 2017 and the master's degree in Naval Architecture and Ocean Engineering from Dalian University of Technology in 2020. He is now a Mechanical Design Engineer in Commercial Aircraft Corporation of China Ltd. His research interests involve in mechanical structural design, mechanical power take-off system, and wave energy.



Yuan Sun is an Associate Professor at Shenyang Institute of automation, Chinese Academy of Sciences. He received his Master's degree (2012) in Ship Engineering from Harbin Engineering University. His research interests include: computational fluid dynamics, underwater unmanned vehicle, and unmanned surface vehicle.



Lei Sun is an Associate Professor at the Dalian University of Technology. He received his Ph.D. (2000) in Port, Coastal and Off-shore Engineering from Dalian University of Technology. His research interests include: marine hydrodynamics, vortex-induced vibration, bubble dynamics, and computational fluid dynamics.



Zhi Zong is a Professor at the Dalian University of Technology. He received his Ph.D. (1995) in Naval Architecture and Ocean Engineering from Hiroshima University. His research interests are in ship hydrodynamics, including ship hydrodynamics in ice, high-performance ships, water waves, underwater explosions, and vortex-induced vibrations.